© 2018. Published by The Company of Biologists Ltd | Journal of Cell Science (2018) 131, jcs204198. doi:10.1242/jcs.204198

RESEARCH ARTICLE

SPECIAL ISSUE: PLANT CELL BIOLOGY

PATELLINS are regulators of auxin-mediated PIN1 relocation and plant development in *Arabidopsis thaliana*

Ricardo Tejos[1], Cecilia Rodriguez-Furlán[2,*], Maciej Adamowski[3], Michael Sauer[4], Lorena Norambuena[2] and Jiří Friml[3,‡]

ABSTRACT

Coordinated cell polarization in developing tissues is a recurrent theme in multicellular organisms. In plants, a directional distribution of the plant hormone auxin is at the core of many developmental programs. A feedback regulation of auxin on the polarized localization of PIN auxin transporters in individual cells has been proposed as a self-organizing mechanism for coordinated tissue polarization, but the molecular mechanisms linking auxin signalling to PIN-dependent auxin transport remain unknown. We used a microarray-based approach to find regulators of the auxin-induced PIN relocation in *Arabidopsis thaliana* root, and identified a subset of a family of phosphatidylinositol transfer proteins (PITPs), the PATELLINs (PATLs). Here, we show that *PATLs* are expressed in partially overlapping cell types in different tissues going through mitosis or initiating differentiation programs. PATLs are plasma membrane-associated proteins accumulated in *Arabidopsis* embryos, primary roots, lateral root primordia and developing stomata. Higher order *patl* mutants display reduced PIN1 repolarization in response to auxin, shorter root apical meristem, and drastic defects in embryo and seedling development. This suggests that PATLs play a redundant and crucial role in polarity and patterning in *Arabidopsis*.

KEY WORDS: PATELLIN, Auxin, *Arabidopsis thaliana*, Auxin transport, Canalization

INTRODUCTION

Multicellular organisms rely on a number of signalling molecules that participate in intracellular, cell-to-cell and long-distance communication, allowing integration of a variety of cellular responses and processes into the tissue context. As sessile organisms, plants have evolved a specific life strategy involving not only physiological but also developmental adaptations to cope with environmental changes. This necessitates mechanisms and signalling molecules that mediate (re)patterning and (re)polarization at the cellular and tissue level to flexibly adjust development. Auxin is a key plant hormone involved in most aspects of plant life, including directional growth responses and formation of new axes of polar growth (Tanaka et al., 2006). Auxin is characteristically distributed in concentration gradients as a consequence of local biosynthesis, intracellular catabolism, and polar cell-to-cell transport (polar auxin transport, PAT) (Benková et al., 2003; Chandler, 2009; Kleine-Vehn et al., 2008; Ruiz Rosquete et al., 2012; Sauer et al., 2013). The direction of PAT is determined by the polarly localized auxin exporters of the PINFORMED (PIN) family (Adamowski and Friml, 2015; Petrášek et al., 2006; Wiśniewska et al., 2006). PIN-mediated auxin transport is feedback regulated by auxin at multiple levels, including transcription, intracellular trafficking, localization and degradation, all of them involving potentially different subsets of auxin receptors and downstream components (Robert et al., 2010; Sauer et al., 2006). Auxin-mediated regulation of PIN localization relies on the nuclear auxin signalling pathway (Sauer et al., 2006) mediated by the auxin receptor TRANSPORT INHIBITOR RESPONSE 1 (TIR1) (Lavy and Estelle, 2016). This suggests that auxin-mediated PIN relocalization involves so far unknown regulator(s), which are in turn transcriptionally controlled via the TIR1 pathway and can be repressed by genes coding for AUX/IAA proteins, such as *AXR3* (Sauer et al., 2006). In order to find these regulators, a microarray-based approach was designed, employing inducible expression of a stabilized AXR3 (also known as IAA17) 'super-repressor' *HS:axr3-1* (Knox et al., 2003), which fails to exhibit auxin-induced PIN relocalization when the repressor transcription is induced. Candidate genes should respond to auxin in the wild type, but not in the *HS:axr3-1* background. Among the candidates, we found few genes coding for phosphatidylinositol transfer proteins (PITPs), the PATELLINs (PATLs), named after the Latin word *patella* or meaning 'small plate', making reference to the subcellular localization of PATL1 at the cell plate during cytokinesis of the founding member of the family in *Arabidopsis* (Peterman et al., 2004). These proteins represent possible candidates for factors that mechanistically link PIN localization with auxin-dependent transcriptional control.

Phosphatidylinositols (PtdIns) are signalling lipid molecules commonly present in all eukaryotic membranes (Balla et al., 2009; Di Paolo and De Camilli, 2006; Meijer and Munnik, 2003). They have a dual cellular function as scaffold lipids to recruit cytosolic proteins, and as precursors of other lipid or soluble second messengers participating in a variety of signalling processes, including stress responses to the environment and during development. Their synthesis is temporally and spatially controlled by metabolic enzymes, such as phosphatases, kinases and phospholipases, allowing fine-tuned lipid levels and responses (Mueller-Roeber and Pical, 2002). In plants, several of the enzymes involved in phosphoinositide metabolism have been characterized in the context of reproductive and vegetative development and during the response to the biotic and abiotic environment. An intriguing group of PtdIns-related proteins are the PITPs, which are

[1]Facultad de Recursos Naturales Renovables, Universidad Arturo Prat, 111093 Iquique, Chile. [2]Plant Molecular Biology Centre, Biology Department, Faculty of Sciences, Universidad de Chile, 7800024 Santiago, Chile. [3]Institute of Science and Technology (IST) Austria, 3400 Klosterneuburg, Austria. [4]Department of Plant Physiology, University of Potsdam, D-14476 Potsdam, Germany.
*Present address: Center for Plant Cell Biology, Institute for Integrative Genome Biology, and Department of Botany and Plant Sciences, University of California, Riverside, California 92521, USA.

‡Author for correspondence (jiri.friml@ist.ac.at)

R.T., 0000-0003-1169-731X; C.R.-F, 0000-0002-3453-4719; L.N., 0000-0002-6031-2394; J.F., 0000-0002-8302-7596

Received 24 March 2017; Accepted 5 July 2017

Journal of Cell Science (2018) 131, jcs204198. doi:10.1242/jcs.204198

represented by the yeast Sec14p protein (Bankaitis et al., 2010). In animal models, PITPs are able to transfer PtdIns or phosphatidylcholine between membranes *in vitro* (Aitken et al., 1990), to stimulate Ca^{2+}-triggered exocytosis (Hay and Martin, 1993), regulate budding and vesicle formation at the trans-Golgi network (Simon et al., 1998), and assist phospholipase C-mediated PtdIns(4,5)P_2 hydrolysis (Cockcroft, 1997; Fensome et al., 1996). Because of these activities, PITPs are placed in a central position at the interphase between phosphoinositide metabolism and signalling (Cockcroft, 2001). However, which one reflects their *in vivo* function is a topic of current investigation.

In plants, several proteomics studies have identified PATLs as putative factors associated with diverse signalling pathways, such as response to brassinosteroid (Deng et al., 2007; Tang et al., 2008) and cytokinin (Černý et al., 2011) hormones, and pathogen attack (Benschop et al., 2007; Elmore et al., 2012; Kiba et al., 2012), the latter supported by functional data on virus mobility and involvement in infectious processes (Kiba et al., 2012; Peiró et al., 2014). PATLs are also involved in cytokinesis (Peterman et al., 2004). However, there is comparatively little direct functional evidence about these genes, and a clear characterization of the PATL subfamily of Sec14p-like proteins in plants is still lacking. Here, we present functional evidence for a redundant role of *Arabidopsis thaliana* PATLs in auxin effect on PIN1 polar localization, and characterise the role of this protein family during plant development based on tissue expression patterns, subcellular localization and higher order mutant analyses.

RESULTS

The auxin feedback on PIN polarity can be visualized by PIN polarity changes in *A. thaliana* root cells manifested by basal-to-inner lateral repolarization of PIN1 in endodermis and pericycle cells, and a basal-to-outer lateral repolarization of PIN2 in cortex cells (Sauer et al., 2006). This effect depends on the SCF^{TIR1}-AUX/IAA-ARF signalling pathway, since ectopic heat shock-inducible expression of a dominant-negative mutant of the auxin signalling repressor AXR3 (HS:*axr3-1*) (Knox et al., 2003) leads to a loss of PIN lateralization after auxin treatment (Sauer et al., 2006). To identify downstream factors required for this auxin effect on PIN polarity, we performed a microarray experiment to search for genes that respond differentially to auxin between wild type and HS:*axr3-1* in roots, and considered those genes as potential mediators of this effect (Fig. S1A; T. Prat, W. Grunewald, G. Molnar, R. Tejos, M. Schmid, M.S. and J.F., unpublished data). The overlap of auxin-regulated genes and genes that are differentially regulated between wild type and HS:*axr3-1* yielded a list of 245 candidate genes that were auxin-regulated in an AXR3-dependent manner, and thus are potential regulators of PIN polarity (Fig. S1B; Table S1). This list was manually examined for genes with a possible role in protein trafficking.

PATLs are auxin-regulated genes required for auxin-mediated PIN1 lateralization

Among the selected genes using this microarray approach, the *PATL* genes appeared to be interesting candidates as they code for phosphoinositide-related proteins that may be involved in auxin-regulated development and PIN protein trafficking and localization, as previously shown for other phosphoinositide-related metabolic enzymes (Ischebeck et al., 2013; Mei et al., 2012; Nováková et al., 2014; Tejos et al., 2014; Ugalde et al., 2016). *PATL2*, *PATL3*, *PATL4* and *PATL6* were found to be differentially represented in response to the auxin microarray data set (Fig. 1A) but these responses were not observed in the HS:*axr3-1* background (Fig. S1C). The auxin regulation of *PATL* genes was confirmed using quantitative RT-PCR (Fig. 1A). *PATL2* and *PATL6* were significantly induced in response to auxin, whereas *PATL3* and *PATL4* were repressed (Fig. 1A). Both responses occurred after 30 and 60 min of auxin treatment (indole 3-acetic acid, IAA; 10 µM). We then tested if PATLs were involved in auxin-mediated PIN1 lateralization in root endodermis cells. To do so, we isolated insertional mutants for *PATL2*, *PATL3*, *PATL4* and *PATL6* (Fig. S2), and as these single *patl* mutants did not show any developmental defect (not shown) we generated higher order mutants. The quadruple *patl2 patl4 patl5 patl6* (*patl2456*$^{-/-}$) mutants displayed clear defects in PIN1 lateralization response, e.g. we observed only limited rearrangement of PIN1 polarity in root endodermis

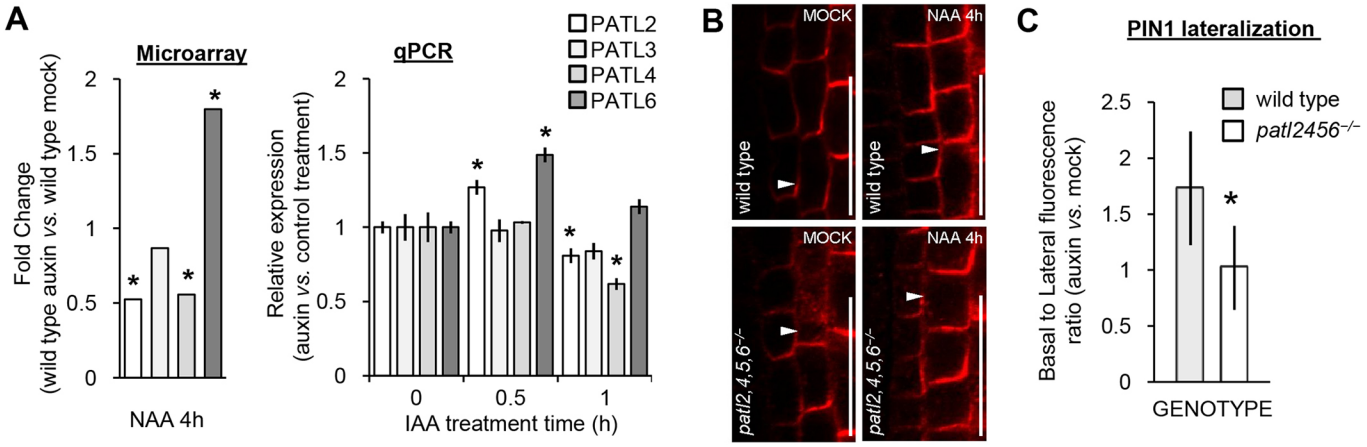

Fig. 1. *PATLs* are auxin-regulated genes involved in auxin-mediated PIN1 repolarization in *Arabidopsis* roots. (A) Left: a subset of the *PATLs* were identified as auxin-modulated genes in the microarray experiment. *PATL2* and *PATL4* were significantly reduced, and the *PATL6* transcript was significantly increased. Fold changes between the conditions are indicated for each gene. **P*<0.05. Right: these data were confirmed using quantitative RT-PCR on plants treated with 10 µM IAA for the indicated time. Data are mean±s.e.m. (*n*=3). **P*<0.05, compared to time zero (Student's *t*-test assuming unequal variance). (B,C) Auxin-induced PIN1 lateralization assay. Seven-day-old wild-type or *patl2456*$^{-/-}$seedlings were treated with 10 µM NAA or 1 µl/ml DMSO (mock control), and PIN1 immunolocalization was performed. Arrowheads in B indicate PIN1 lateralization (red signal) in root endodermis cells. The basal to inner lateral ratio was measured for PIN1 fluorescence in root endodermis cells using ImageJ, and the mean±s.d. for *n*=35 individual cells corresponding to 10 different roots was calculated for each genotype (C). The experiment was repeated twice. **P*<0.05, comparing wild type to *patl2456*$^{-/-}$ mutants (two-tailed Student's *t*-test). Scale bars: 20 µm.

Journal of Cell Science (2018) 131, jcs204198. doi:10.1242/jcs.204198

following auxin treatment (1-naphthaleneacetic acid, NAA; 10 µM) (Fig. 1B,C). However, PIN2 lateralization response in *patl2456*$^{-/-}$ mutants was comparable to that in the wild type. Additionally, PIN1 and PIN2 localization in normal conditions did not show obvious defects in *patl2456*$^{-/-}$ mutants. This provided further confirmation that PATLs are good candidates for regulators of auxin effect on PIN1 polarity identified from our microarray approach.

The *A. thaliana* PITP family

PATLs belong to a family of proteins having a domain homologue to yeast Sec14p (Peterman et al., 2004; Vincent et al., 2005). *Sec14* is one of the 24 complementation groups of *Saccharomyces cerevisiae secretory* (*Sec*) mutants isolated by Novick and co-workers in the early 1980s (Novick and Schekman, 1979; Novick et al., 1980, 1981), and Sec14p was later demonstrated as an essential protein that functions in the formation and exit of vesicles from the trans-Golgi network (Bankaitis et al., 1990). In order to identify all *Arabidopsis* PITPs, we used the yeast Sec14p protein sequence to search The Arabidopsis Information Resource (TAIR) database for proteins with significant homology, and found a total of 32 Sec14p-like proteins (Table S2) that group into two distinct phylogenetic clades (Fig. 2A). Some of them (14/32) consist solely of a Sec14p-like domain, similar to the yeast Sec14p protein organization, while others have incorporated an additional domain (Fig. 2B) (Mousley et al., 2007). The *A. thaliana* Sec Fourteen Homologs (AtSFHs) group in a single cluster (Fig. 2A) and have a relatively high homology to the yeast Sec14p (37–43% homology, Table S2). In addition to the Sec14p-like domain, 12 of 14 of the AtSFHs contain a 100 amino acid-long nodulin domain at their C-terminal end. This domain was initially characterized in the nodule-specific protein Nlj16 and defines a plasma membrane (PM)-targeting module (Kapranov et al., 2001). The second cluster is formed by a heterogeneous group of proteins with a variable homology to Sec14p (21–32% homology) (Table S2). We have called them *A. thaliana* PITPs (AtPITPs). This cluster contains, among others, the *PATL* gene subfamily, a subclade of six proteins containing a Golgi dynamics (GOLD) domain in tandem with the Sec14p-like domain (Fig. 2B). The GOLD domain is widely present among mammalian proteins associated to membranes by hydrophobic interactions that participate in vesicle formation at the ER/Golgi interphase. It is also found in proteins that modulate membrane homeostasis (Anantharaman and Aravind, 2002). Similarly, as occurs for many other protein families in plants, PITPs in *Arabidopsis* have greatly expanded in number and diversified in their function. The few published studies on plant PITPs implicated their function in response to abiotic (Kearns et al., 1998; Monks et al., 2001) and biotic (Kiba et al., 2012; Peiró et al., 2014) stresses during nodule formation (Kapranov et al., 2001), cell division (Peterman et al., 2004) and subcellular trafficking (Böhme et al., 2004; Vincent et al., 2005), which suggests a broad spectrum of functions regulated by PITPs in plants.

PATL expression and protein localization patterns

Expression and protein localization patterns for the *Arabidopsis* PATLs have been addressed by just a few studies (Peterman et al., 2004; Suzuki et al., 2016). PATL1 and PATL2 have been shown to bind phosphoinositides, and both proteins have been observed to form cell plates in the root apical meristem (RAM) using specific antibodies (Peterman et al., 2004), or through constitutive expression of GFP-fusion proteins (Suzuki et al., 2016). Additionally, both PATL1 and PATL2 were localized in tobacco BY-2 cells and observed to be closely associated with the periphery

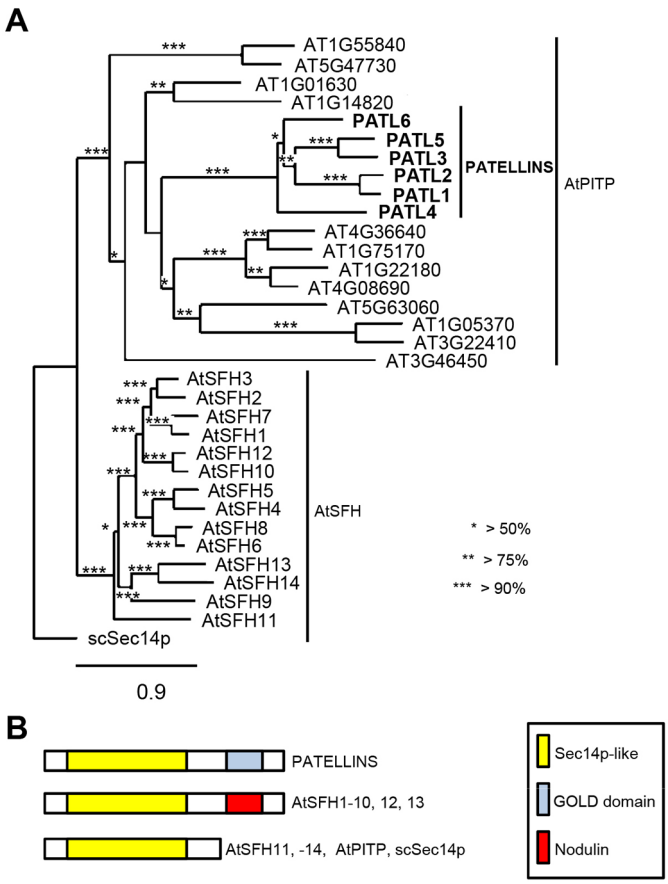

Fig. 2. Sec14-like proteins in *A. thaliana*. (A) Phylogenetic tree of Sec14p-like proteins from *Arabidopsis*. *S. cerevisiae* Sec14p (scSec14p) was used as the outgroup. The *Arabidopsis* proteins group in two clades, one highly homologous to scSec14p-containing proteins (AtSFH1–14), which seem to be evolutionarily older and less diverse, although two of them do not contain an extra nodulin-like domain (AtSFH11 and AtSFH14). The second clade contains a more diverse group of PITPs in terms of homology to scSec14p (see Table S2). Within this group appears a small cluster of six proteins that contain an additional GOLD domain, the PATLs. (B) Schematic of the protein configuration found among *Arabidopsis* PITPs. A Sec14p-like domain (yellow box) can be found in tandem with a GOLD domain (blue box) or a nodulin-like domain (red box), or it can be the only distinguishable protein domain, as is the case for scSec14p.

of the cell plates, confirming the close relationship between PATL proteins and membrane trafficking during the formation of cell plates, a known phosphoinositide-dependent membrane trafficking process (Isono et al., 2010; Suzuki et al., 2016; van Leeuwen et al., 2007; Vermeer et al., 2006). On the other hand, PATL3 and PATL6 have been ectopically expressed as GFP fusions in leaf pavement cells and they localize to the PM, forming discrete clusters (Peiró et al., 2014). However, there are no available data about the cell- or tissue-specific regulation of PATL expression.

To obtain additional insight into PATL expression pattern and function, we generated *Arabidopsis* translational reporter lines for the *PATL* genes identified in the microarray experiment (see Fig. 1; Fig. S1). To do so, we used native promoters (2000 bp of their gene regulatory region) to drive the expression of the GFP coding gene fused to the 5′-end of the full-length coding sequences of *PATL2*, *PATL3*, *PATL4* and *PATL6*, and generated *Arabidopsis* transgenic plants. We then used those lines to observe embryogenesis, and to assess 7- to 12-day-old seedlings for GFP-PATLs, to gain insight into their expression patterns and protein localization in embryos, RAM

Journal of Cell Science (2018) 131, jcs204198. doi:10.1242/jcs.204198

and lateral root primordia (LRP), as they represent tissues in which PIN-dependent local auxin accumulation has been proposed to play an important role (Adamowski and Friml, 2015). We observed that in the analysed tissues, PATLs are expressed in distinct, sometimes partly overlapping patterns. Their expression is linked mainly to the leaf pavement cells, vascular tissue and dividing cells of the RAM, and at all stages of LRP development, and are observed during embryogenesis (Figs 3 and 4). For instance, as previously shown, PATL1 is expressed in the whole RAM associated with the cell plates (Fig. 3A) (Peterman et al., 2004), and in stele cells in the distal zone of the RAM, where cells cease dividing and start to differentiate (Fig. 3B, asterisk). PATL2p:GFP-PATL2 was observed in pericycle and provascular cells in the distal zone of RAM (Fig. 3C,D) as well as in differentiated vascular tissues in roots (Fig. 3C,E), partially resembling the PATL1 expression pattern (Fig. 3A). Additionally, PATL2p:GFP-PATL2 was observed in pericycle cells in the root elongation zone (Fig. 3C,D) and from stage V onwards during LRP formation (Fig. 3F; LRP developmental stages as described by Malamy and Benfey, 1997), in the vascular phloem tissues and in the cells flanking the developing LRP (Fig. 3E,F). The potential involvement of PATL2 in vascular development was also suggested by PATL2p:GFP-PATL2 expression during early specification of provascular tissues during embryogenesis (Fig. 4A).

PATL3, PATL4 and PATL6 expression and localization are closely associated with tissues with high mitotic activity, including the RAM, LRP, embryo and stomata precursor cells. PATL3p:GFP-PATL3 expression is more prominent in external cell layers (i.e. the epidermis and cortex in root tips) (Fig. 3G) compared to the more ubiquitous expression of PATL4p:GFP-PATL4 in RAM (Fig. 3J), and the stele cell expression of PATL6p:GFP-PATL6 (Fig. 3O). Additionally, PATL3p:GFP-PATL3 and PATL4p:GFP-PATL4 are expressed in the basal meristem of the root tip (Fig. 3G,H,J,K), and the LRP (Fig. 3I, N), and they accumulate at the anticlinal PM of the newly divided cells (Fig. 3H,L,P, arrowheads). This partially overlapping and complementary PATL expression found in root tissues was also observed in embryogenesis, and pavement cell and stomata development in cotyledon epidermis (Fig. 4). For instance, in embryos, PATL2p:GFP-PATL2 is expressed in provascular cells (Fig. 4A), whereas PATL4p:GFP-PATL4 expression appears to be ubiquitous during early embryogenesis stages, localizing mostly to the cytosol (Fig. 4B, left panel), but becomes concentrated at the PM in later stages (Fig. 4B, right panel). Furthermore, PATL6p:GFP-PATL6 is only expressed in the inner provascular cell layers in embryos (Fig. 4C). Notably, in cotyledon epidermis, PATL2p:GFP-PATL2, PATL4:GFP-PATL4 and PATL6p:GFP-PATL6 are also expressed in different cell types with a limited overlap (Fig. 4D–F). These distinct expression patterns point to a developmentally regulated expression, in particular in highly dividing tissues, as previously shown for PATL1 (Peterman et al., 2004), but also indicate their potential involvement in differentiation processes of vascular tissues, lateral roots and stomata. Moreover, these observations point to common roles for PATLs linked to their PM association. Indeed, when overexpressed, PATL1–5 localized to the PM with some level of apical/basal enrichment, possibly due to their strong localization to the cell plate during cytokinesis (Fig. S3). Taken together, these observations suggest that all members of the PATL family associate with the PM, showing tissue- and cell type-specific expression patterns.

PATLs are redundantly required for auxin-mediated root development

To address the role of PATLs during plant development, we isolated knockout mutants for *PATL2*, *PATL4*, *PATL5* and *PATL6* and a single knockdown mutant for *PATL3* (Fig. S2) from the Salk collection (Alonso et al., 2003). No developmental abnormalities were detected in roots in single, double and triple mutant combinations (not shown), indicating a pronounced functional redundancy among the *PATL* gene family. Nonetheless, in the multiple *patl2456*$^{-/-}$ mutant, the RAM size was reduced by 25% (Fig. 5A,B). Auxin regulates several processes in the root, including cell division and elongation, meristem size in a concentration-dependent manner, and root gravitropism (Lavy and Estelle, 2016; Ruzicka et al., 2009). Therefore, we evaluated auxin response in *patl2456*$^{-/-}$ mutants germinating seeds in media containing 2,4-dichlorophenoxyacetic acid (2,4D), a synthetic auxin analogue. In wild-type plants, 2,4D reduces RAM size at 10 and 100 nM concentrations, whereas *patl2456*$^{-/-}$ mutants were resistant to this inhibitory effect at 10 nM (Fig. 5C). Both 2,4D concentrations, 10 and 100 nM, did not perturb normal primary root gravitropism in wild-type seedlings, but *patl2456*$^{-/-}$ mutants germinated in 100 nM 2,4D were highly agravitropic (Fig. 5D). These data indicate that PATLs are involved in auxin-regulated processes including root meristem size and gravitropic growth.

PATLs are redundantly required for embryo and seedling patterning

We further characterized *patl2456*$^{-/-}$ mutants by evaluating other developmental phenotypes, as suggested by the expression patterns described in Figs 3 and 4. As PATL2, PATL4 and PATL6 are expressed during embryo development, we analysed the *patl2456*$^{-/-}$ mutants for defects in early embryogenesis, during which auxin and auxin transport play a major role (Jeong et al., 2011; Petrášek and Friml, 2009; Robert et al., 2015). *Arabidopsis* embryogenesis follows a highly stereotypic division pattern. After zygote formation, an initial asymmetric division generates a small apical cell and a larger basal cell. The basal cell further divides anticlinally into a cell file, the suspensor, and the apical cell develops to form an embryo body. Later during embryogenesis, the uppermost suspensor cell, the hypophysis, is included in the embryo body as an auxin-dependent founder of the root meristem (Robert et al., 2013; Smit and Weijers, 2015) (Fig. 6A–F). When we analysed the *patl2456*$^{-/-}$ mutants, ∼10% of the embryos (n=205) showed aberrant cell divisions of the hypophysis (compare Fig. 6G,H with Fig. 6B,C). Next, we introduced the *patl3* mutant into the quadruple *patl2456*$^{-/-}$ mutant. Notably, 4.8% of the embryos (n=167) obtained from *patl2*$^{+/-}$ *patl3456*$^{-/-}$ mutant plants displayed aberrant morphology at basal or apical poles (Fig. 6I–K). A segregation distortion for the *patl2* mutant allele in the progeny of *patl2*$^{+/-}$*patl3456*$^{-/-}$ plants was observed when compared to the segregation of a normal Mendelian gene (Table S3). So, we hypothesized that the quintuple mutant was partially lethal as we found developmental phenotypes such as very tiny seedlings (Fig. 7A), as well as rootless and mono- or triple-cotyledon seedlings (Fig. 7B–E) segregating at a frequency of 4.6% (n=151) (much below the expected 25% frequency), when we analysed the progeny of a single *patl2*$^{+/-}$ *patl3456*$^{-/-}$ plant (Table S3).

To independently interfere with the function of a PATL subfamily, we generated artificial microRNAs (amiRNAs) targeting *PATL1* and *PATL3*, and introduced the constructs into a quadruple *patl2456*$^{-/-}$ mutant plant. We then crossed T2 transformants and analysed the first generation of that cross. In the first generation, ∼25% (n=75) of *patl2456*$^{-/-}$ *amiPATL1/3* seedlings showed phenotypes similar to that described for *patl2*$^{+/-}$*patl3456*$^{-/-}$ mutants, including cotyledon defects (Fig. 7F,G), rootless seedlings (Fig. 7H), and seedlings with ectopic structures (Fig. 7I). Altogether,

Journal of Cell Science (2018) 131, jcs204198. doi:10.1242/jcs.204198

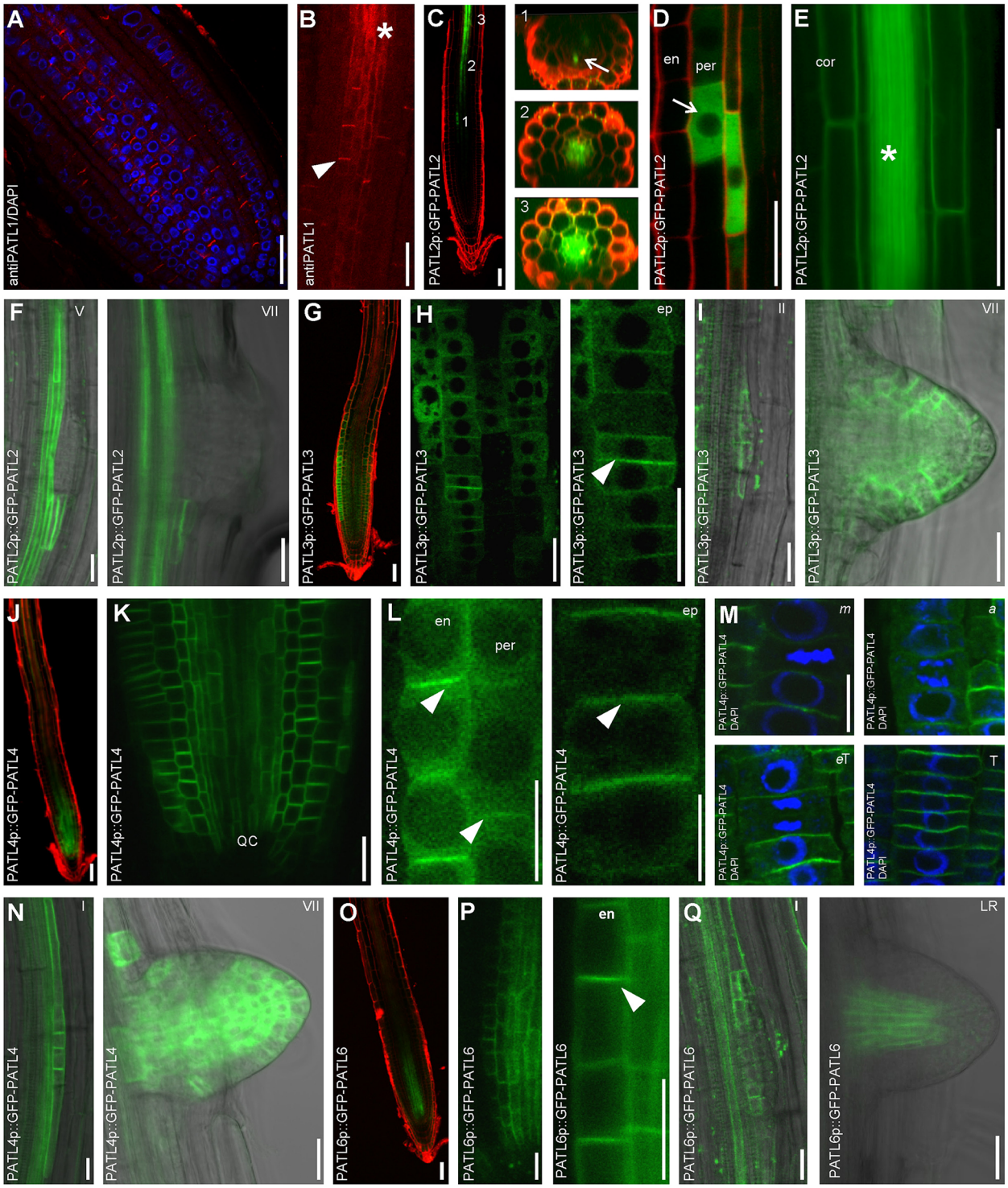

Fig. 3. *PATL* expression patterns and subcellular localization in *Arabidopsis* roots. (A–Q) Expression patterns were obtained with a confocal microscope using immunohistochemical assays for PATL1 in wild-type roots (A,B) or using GFP-PATL translational reporter lines (C–Q). (A,B) PATL1 expression in RAM (A) and in inner vascular tissue in the differentiation zone in root tips (B, asterisk) in wild-type seedlings. PATL1 was detected using an anti-PATL1 antibody (red). Nuclei were stained using 1 µg/ml DAPI (blue). (C–F) PATL2p:GFP-PATL2 expression pattern (green) in primary roots can be observed in the distal zone of the RAM in pericycle cells (D, arrow), in vascular tissue in mature roots (C,E, asterisk), and in the LRP (F). In the right panels in C, *z*-stack reconstructions tilted 90° in the *x*-axis are shown from the areas labelled 1–3 in the left panel in C. (G–I) *PATL3p:GFP-PATL3* expression pattern in primary root (G,H) and LRP (H). The arrowhead in H indicates GFP-PATL3 at the newly formed cell plate of an epidermal cell. (J–N) *PATL4p:GFP-PATL4* was observed in all layers of primary roots (J) with the exception of the quiescent centre (K). GFP-PATL4 is localized at the apical PM of two contiguous cells (L, arrowheads), and is enriched at later stages of cell division (mitosis stages indicated in the upper right corner of the panels in M). GFP-PATL4 expression was observed during all stages of LRP development (N). (O–Q) *PATL6p:GFP-PATL6* expression pattern in primary roots (P) and LRP (Q). The arrowhead in P indicates polar enrichment of GFP-PATL6 in endodermal cells. The LRP developmental stages are indicated in the upper right corner of each image in F, I and N. DAPI was used to stain nuclei (blue in A,M) and propidium iodide was used to counterstain cell walls in root cells (red in C,G,J,O). Scale bars: 20 µm. a, anaphase; cor, cortex; en, endodermal cell; ep, epidermal cell; eT, early telophase; m, metaphase; per, pericycle cell; QC, quiescent centre; T, telophase.

Journal of Cell Science (2018) 131, jcs204198. doi:10.1242/jcs.204198

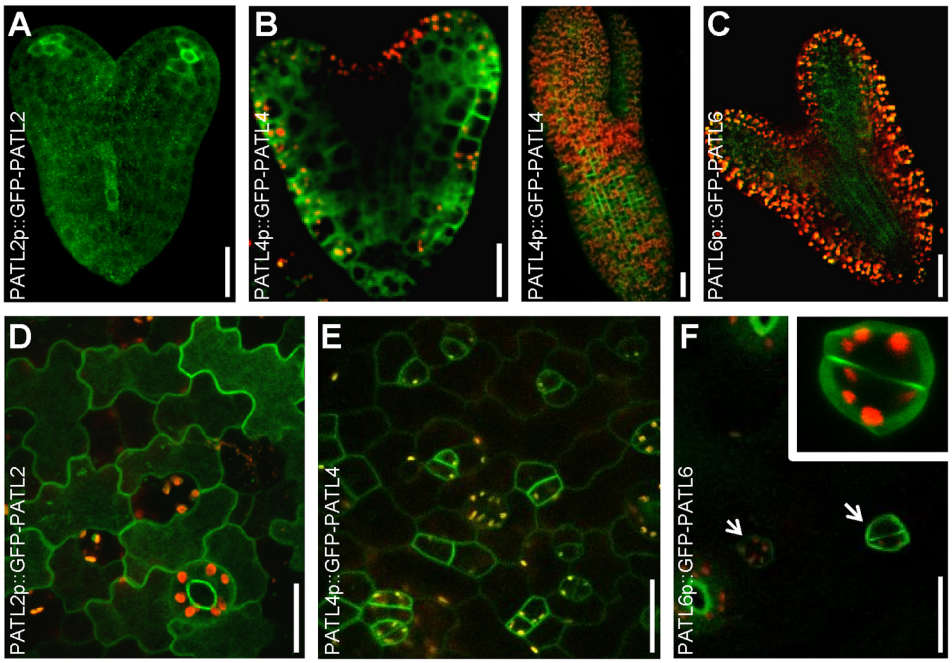

Fig. 4. *PATL* expression during embryogenesis and in cotyledon epidermal cells. *PATL* expression during embryo development (A–C) and in cotyledon epidermal cells (D–F) was observed using *PATL2p:GFP-PATL2* (A,D), PATL4p:GFP-PATL4 (B,E), and *PATL6p:GFP-PATL6* (C,F) reporter lines. GFP fluorescence is depicted in green and chloroplast autofluorescence in red. Scale bars: 20 µm.

these observations suggest a crucial and redundant function for PATLs in embryo patterning and organogenesis.

DISCUSSION

This work is the first attempt to describe the function of the family of the *Arabidopsis* GOLD-containing Sec14p-like proteins, the PATLs. We identified multiple members of this family as potentially auxin-regulated genes from the microarray approach designed to obtain regulators of PIN polarity and auxin feedback on PIN polarity, acting downstream of TIR1-AUX/IAA-ARF auxin signalling.

The results presented here indicate that PATL overlapping expression patterns are developmentally regulated. PATLs are expressed in tissues with high cell division activity, such as RAM and LRP, or those entering a differentiation program, such as vascular tissue formation and stomata development. *PATL* expression patterns closely resemble *PIN* expression patterns. For instance, *PATL6* and *PIN1* are both expressed in stele cells in root tips (Fig. 3O,P) (Omelyanchuk et al., 2016); *PATL4* and *PIN1*, and *PATL2* and *PIN6*, are co-expressed in LRP (Fig. 3N,Q) (Benková et al., 2003). Additionally, PINs and PATLs also share expression in other tissues such as root epidermis and cortex, and in embryos. Therefore, in addition to the described localization and putative function of PATL1 and PATL2 during late cell plate formation (Peterman et al., 2004), they may be involved in regulating other lipid-based signalling pathways at the PM implicated in regulating PIN1 proteins, or other proteins and processes linked to cell function and differentiation.

Our genetic analysis revealed that PATLs have crucial and redundant functions in plant development. Knocking out four of the six *PATL* genes (*patl2456*$^{-/-}$) produces mild defects during embryonic root patterning at low frequency. When only one *PATL* gene remained expressed in the quintuple mutant background, stronger phenotypes in apical-basal patterning were observed, and many embryos did not produce viable seeds. The surviving seeds produced seedlings with strong patterning defects often lacking roots and showing their regular formation of cotyledons. Even stronger phenotypes along the same lines were observed when the function of all six members was downregulated. These strong patterning phenotypes were strongly reminiscent of mutants in auxin transport (such as *pin1* or *pin1,3,4,7*) (Benková et al., 2003; Friml et al., 2003), signalling (such as *monopteros* or *bodenlos*) (Weijers et al., 2006) or PIN polar localization (*gnom*, *pinoid*) (Kleine-Vehn et al., 2009). These strong, apparently auxin-related patterning phenotypes, together with defective auxin effect on PIN polarity and auxin-related growth phenotypes in the *patl2456*$^{-/-}$ roots, support the notion that PATLs are components of the auxin feedback on PIN polarity.

Previous experiments have indicated a role for phosphoinositide in auxin signalling (Xue et al., 2007). In this report, we identified the PATLs as potential molecular intermediates in an auxin-mediated transcriptional control of key enzymes involved in the interphase between lipid synthesis and lipid signalling. PATLs are associated with the PM, where they may regulate the levels and localization of phosphoinositides. In this way, PATLs would influence signalling cascades by directly or indirectly controlling different PM proteins, including PIN auxin transporters. The exact molecular base of these regulations and how they are integrated with other components of the auxin signalling and PIN polarity control remain topics for future investigation.

MATERIALS AND METHODS

Plant material

All lines are in the Columbia background of *A. thaliana.* Insertional mutants *patl2* (SALK_086866), *patl3* (SALK_093994), *patl4* (SALK_139423), *patl5* (SALK_124448) and *patl6* (SALK_099090) were obtained from Arabidopsis Biological Research Center (ABRC) and genotyped for homozygosity using the primers listed in Table S4. Seeds were surface sterilized overnight by chlorine gas, sown on solid Arabidopsis MS medium [0.5× Murashige and Skoog basal salts, 1% (w/v) sucrose and 0.8% (w/v) agar, pH 5.9] and stratified at 4°C for at least 2 days prior to transfer to a 16 h-light–8 h-dark illumination regime in a growth room kept at 22°C. Seedlings were grown vertically for 4–12 days prior to the analysis.

Cloning procedures

Coding sequences for PATLs as well as promoter sequences corresponding to 2000 bp upstream of the ATG codon were amplified using iPROOF DNA polymerase (BioRad), cloned using pENTR Directional TOPO Cloning Kit (Invitrogen) or Gateway BP Clonase (Invitrogen), and recombined into

Journal of Cell Science (2018) 131, jcs204198. doi:10.1242/jcs.204198

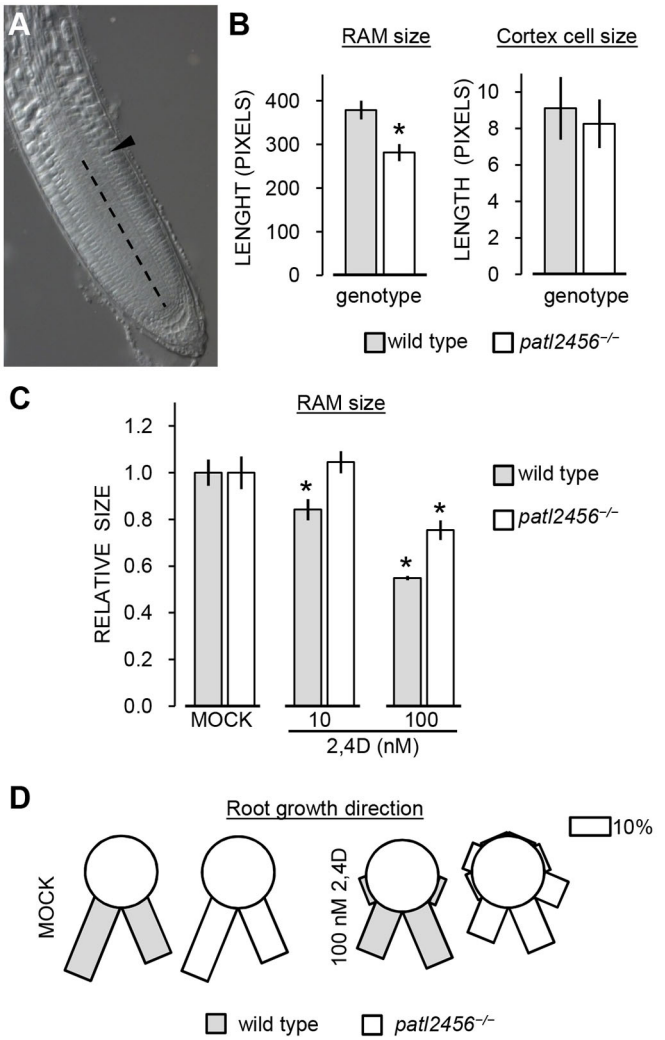

Fig. 5. *patl2456*$^{-/-}$ mutants have reduced RAM size and perturbed response to auxin. (A–C) RAM was measured using images obtained from 7-day-old seedling root tips mounted in chloral hydrate using a DIC microscope. The RAM was measured from the quiescent centre to the point at which the epidermal cells started to elongate, i.e. were significantly larger (arrowhead in A). *patl2456*$^{-/-}$ mutants have a shorter RAM than wild-type seedlings (B) and are resistant to 10 nM 2,4D (C). In B and C, data are mean± s.e.m. of three biological repeats. **P*<0.05 (unpaired Student's *t*-test in B; two-way ANOVA and Tukey's multiple comparison tests in C). (D) Root tip growth direction in wild-type and *patl2456*$^{-/-}$ mutant seedlings germinated in the presence of 0.1 µM 2,4D. Root tip direction was evaluated in seedlings 7 days postgermination. Data were gathered using ImageJ software and clustered into eight bins representing the tip direction (*n*>45).

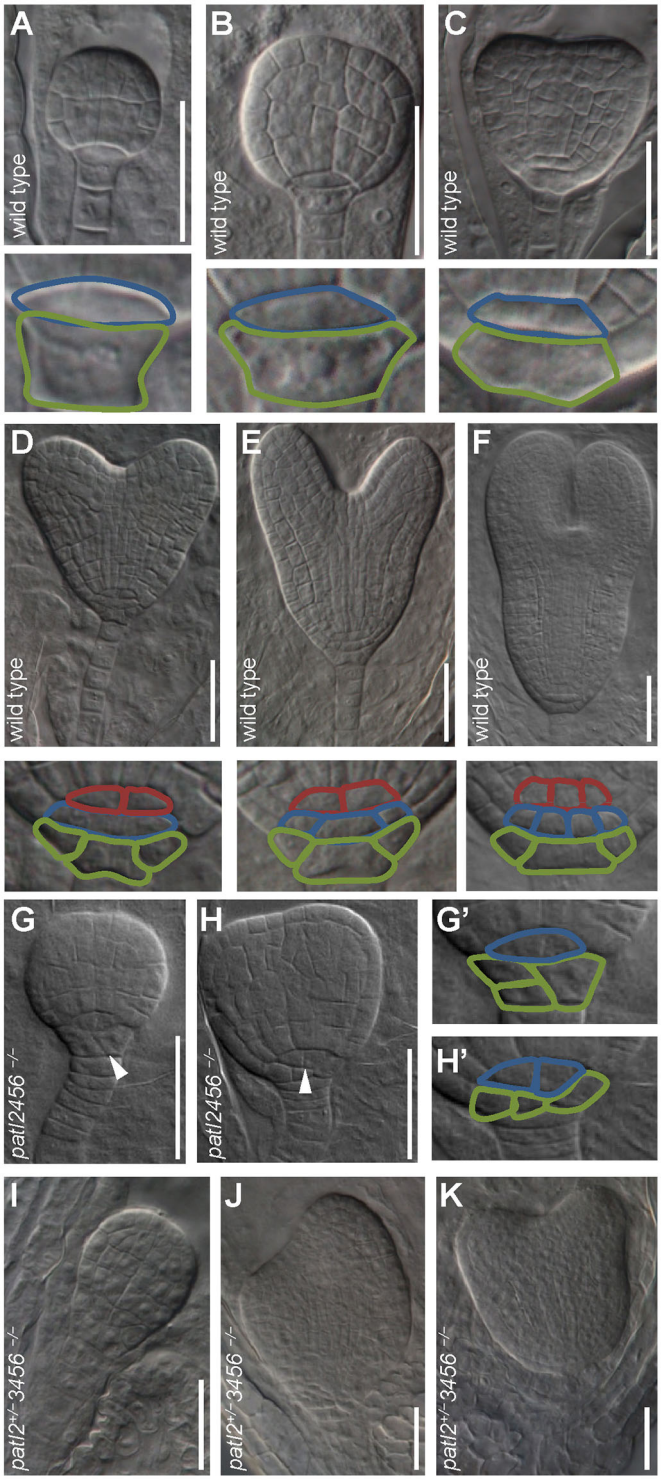

Fig. 6. PATLs regulate embryo patterning. (A–F) Embryo development in the wild type and the normal division patterns during basal pole formation (insets). (G–H′) *patl2456*$^{-/-}$ mutant embryos displaying abnormal division planes. Notice the additional divisions in both cases (arrowheads in G,H). (I–K) Images of mutant embryos obtained from *patl2*$^{+/-}$*patl3456*$^{-/-}$ plants. They show defects in basal (I) or apical poles (J), as well as an abnormal morphology at cotyledons (K). Scale bars: 1 mm.

destination expression vectors as previously described (Karimi et al., 2007). All forward primers for cloning coding sequences contained the attB1 sequence 5′-GGGGACAAGTTTGTACAAAAAAGCAGGCTTC-3′ upstream of the gene-specific sequence, and all reverse primers contained the attB2 sequence 5′-GGGGACCACTTTGTACAAGAAAGCTGGGTC-3′ upstream of the gene-specific sequence. Similarly, forward primers for cloning promoter sequences contained the attB4 sequence 5′-GGGGACAACTTTGTATAGAAAAGTTGGA-3′, and reverse primers the attB1r adapter sequence 5′-GGGGACTGCTTTTTTGTACAAACTTGC-3′. All sequence-specific primers used for cloning are listed in Table S4.

AmiRNAs were designed using Web MicroRNA Designer (Ossowski et al., 2008; http://wmd3.weigelworld.org/cgi-bin/webapp.cgi). Briefly, we used full *PATL1* and *PATL3* coding sequences, selected for each gene two amiRNA sequences from the list of sequences suggested by the web designer (PATL1a, 5′-TATAGTGTAGTTTGCTGGCGG-3′; PATL1b, 5′-TCGAATTGTTTAACAGCCCGT-3′; PATL3a, 5′-TGTCTTATTATAAAGCTCCGT-3′; PATL3b, 5′-TACACATAAGATATCTCGCTT-3′), and generated two amiRNAs following a PCR-based approach to generate point mutations in the

Journal of Cell Science (2018) 131, jcs204198. doi:10.1242/jcs.204198

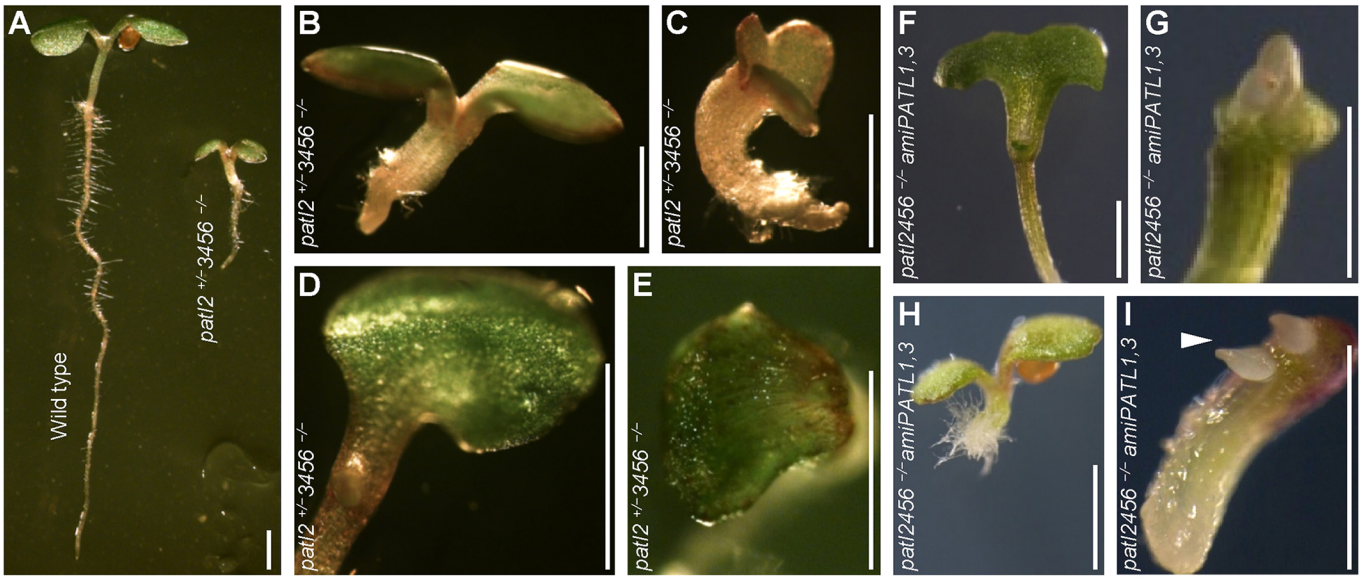

Fig. 7. Seedling phenotypes in *patl* multiple mutants. (A–E) Abnormal seedlings segregating in the progeny of a *patl2*$^{+/-}$*patl3456*$^{-/-}$ plant. Four-day-old wild-type seedlings (A, left) are noticeably bigger than 4.6% (*n*=151) of *patl* mutants (A, right). Rootless seedlings (B,C), and seedlings with cotyledon phenotypes such as tricotyledons (C) and monocotyledons (D,E), appeared in 3% of the cases (*n*=371) of *patl2*$^{+/-}$*patl3456*$^{-/-}$ plants. Scale bars: 1 mm. (F–I) Mutant seedlings resulting from a cross between two homozygous plants (*patl2456*$^{-/-}$ amiPATL1 and *patl2456*$^{-/-}$ amiPATL3). We observed seedlings displaying fused cotyledons (F), defective cotyledons (G) and rootless seedlings (H), as well as a drastically deformed seedling with only a couple of leaf primordia-like structures (arrowhead in I). Scale bars: 1 mm.

microRNA precursor MIR319a (plasmid template pRS300). Then, the produced amiRNA sequences were cloned using Gateway technology and recombined to expression vectors containing the strong constitutive promoter RPS5a and transformed by the floral dip method into the quadruple homozygous *patl* mutant (*patl2456*$^{-/-}$). After selection of the transgenic plants, *patl2456*$^{-/-}$ *amiPATL1* and *patl2456*$^{-/-}$ *amiPATL3* were crossed to generate a multiple *patl* mutant *patl2456*$^{-/-}$ *amiPATL1/3*.

Expression analysis

Total RNA was extracted with the RNeasy Mini kit (Qiagen). Isolated RNA was treated with DNase I recombinant (Roche) to remove contaminating genomic DNA. For the RT-PCR reactions, Poly(dT) cDNA was prepared from 1 µg total RNA with an iScript cDNA synthesis kit (BioRad). PCR conditions were as follows: the PCR mix was heated for 5 min to 95°C, followed by 30 cycles of denaturation for 30 s at 95°C, annealing at 57°C for 30 s and extension for 60 s at 72°C. As housekeeping gene, the expression of the constitutive gene *ACTIN 8* (AT1G49240) was used. All primers used are listed in Table S4.

Immunolocalization and microscopy

Primary root and embryo immunolocalization was performed as described by Sauer et al. (2006) using an automatized alternative. Antibodies were diluted 1:1000 for rabbit anti-PIN1 (Paciorek et al., 2005) and rabbit anti-PATL1 (Peterman et al., 2004), and 1:600 for rabbit anti-GFP (Molecular Probes) and the secondary rabbit anti-IgG conjugated to Cy3 (Sigma-Aldrich). For measuring the RAM, the root tips were mounted in chloral hydrate and visualized using an Olympus BX51 DIC microscope. For live imaging, seedlings at 4 days after germination were mounted in a drop of liquid Arabidopsis MS medium and visualized immediately. All confocal pictures were taken with a Zeiss CSLM 710 confocal microscope. Quantifications of PIN1 auxin lateralization were performed using the ImageJ software freely available at http://imagej.nih.gov/ij/, as previously published (Sauer et al., 2006).

Phylogenetic analysis

All *Sec14p*-like genes in *Arabidopsis* were identified using the BLAST tool from TAIR (http://www.arabidopsis.org/Blast/index.jsp), with yeast Sec14p (scSec14p; YMR079W) as the query sequence. 32 *Arabidopsis* proteins appeared as having some degree of homology to scSec14p (Table S2). Phylogenetic analysis was performed using the web-based tool freely available at http://www.phylogeny.fr, and the MUSCLE alignment and neighbour-joining method with 100 bootstraps.

Acknowledgements

We are grateful to Prof. Kaye T. Peterman for her kind gift of anti-PATL1 antibodies and to Prof. Aliro Villacorta for helpful discussions.

Competing interests

The authors declare no competing or financial interests.

Author contributions

Conceptualization: R.T., M.S., J.F.; Investigation: R.T., C.R.-F., M.A., M.S., L.N.; Resources: J.F.; Writing - original draft: R.T.; Writing - review & editing: R.T., C.R.-F., M.S., L.N., J.F.; Funding acquisition: J.F.

Funding

This work was supported by the European Research Council (ERC-2011-StG 20101109-PSDP).

Data availability

Raw microarray data from this article can be found in the EMBL ArrayExpress repository under accession number E-MEXP-3283 (https://www.ebi.ac.uk/arrayexpress/experiments/E-MEXP-3283/).

Supplementary information

Supplementary information available online at
http://jcs.biologists.org/lookup/doi/10.1242/jcs.204198.supplemental

References

Adamowski, M. and Friml, J. (2015). PIN-dependent auxin transport: action, regulation, and evolution. *Plant Cell* **27**, 20-32.

Aitken, J., Paul, G., van Heusden, G. P. H., Temkin, M. and Dowhan, W. (1990). The gene encoding the phosphatidylinositol transfer protein is essential for cell growth. *J. Biol. Chem.* **265**, 4711-4717.

Alonso, J. M., Stepanova, A. N., Leisse, T. J., Kim, C. J., Chen, H., Shinn, P., Stevenson, D. K., Zimmerman, J., Barajas, P., Cheuk, R. et al. (2003). Genome-wide insertional mutagenesis of Arabidopsis thaliana. *Science* **301**, 653-657.

Anantharaman, V. and Aravind, L. (2002). The GOLD domain, a novel protein module involved in Golgi function and secretion. *Genome Biol.* **3**, research0023.

Balla, T., Szentpetery, Z. and Kim, Y. J. (2009). Phosphoinositide signaling: new tools and insights. *Physiology (Bethesda)* **24**, 231-244.
Bankaitis, V. A., Aitken, J. R., Cleves, A. E. and Dowhan, W. (1990). An essential role for a phospholipid transfer protein in yeast Golgi function. *Nature* **347**, 561-562.
Bankaitis, V. A., Mousley, C. J. and Schaaf, G. (2010). The Sec14 superfamily and mechanisms for crosstalk between lipid metabolism and lipid signaling. *Trends Biochem. Sci.* **35**, 150-160.
Benková, E., Michniewicz, M., Sauer, M., Teichmann, T., Seifertová, D., Jürgens, G. and Friml, J. (2003). Local, efflux-dependent auxin gradients as a common module for plant organ formation. *Cell* **115**, 591-602.
Benschop, J. J., Mohammed, S., O'flaherty, M., Heck, A. J. R., Slijper, M. and Menke, F. L. H. (2007). Quantitative phosphoproteomics of early elicitor signaling in Arabidopsis. *Mol. Cell. Proteomics* **6**, 1198-1214.
Böhme, K., Li, Y., Charlot, F., Grierson, C., Marrocco, K., Okada, K., Laloue, M. and Nogué, F. (2004). The Arabidopsis COW1 gene encodes a phosphatidylinositol transfer protein essential for root hair tip growth. *Plant J.* **40**, 686-698.
Černý, M., Dyčka, F., Bobálová, J. and Brzobohatý, B. (2011). Early cytokinin response proteins and phosphoproteins of Arabidopsis thaliana identified by proteome and phosphoproteome profiling. *J. Exp. Bot.* **62**, 921-937.
Chandler, J. W. (2009). Local auxin production: a small contribution to a big field. *BioEssays* **31**, 60-70.
Cockcroft, S. (1997). Phosphatidylinositol transfer proteins: requirements in phospholipase C signaling and in regulated exocytosis. *FEBS Lett.* **410**, 44-48.
Cockcroft, S. (2001). Phosphatidylinositol transfer proteins couple lipid transport to phosphoinositide synthesis. *Semin. Cell Dev. Biol.* **12**, 183-191.
Deng, Z., Zhang, X., Tang, W., Oses-Prieto, J. A., Suzuki, N., Gendron, J. M., Chen, H., Guan, S., Chalkley, R. J., Peterman, T. K. et al. (2007). A proteomics study of brassinosteroid response in Arabidopsis. *Mol. Cell. Proteomics* **6**, 2058-2071.
Di Paolo, G. and De Camilli, P. (2006). Phosphoinositides in cell regulation and membrane dynamics. *Nature* **443**, 651-657.
Elmore, J. M., Liu, J., Smith, B., Phinney, B. and Coaker, G. (2012). Quantitative proteomics reveals dynamic changes in the plasma membrane during Arabidopsis immune signaling. *Mol. Cell. Proteomics* **11**, M111.014555.
Fensome, A., Cunningham, E., Prosser, S., Tan, S. K., Swigart, P., Thomas, G., Hsuan, J. and Cockcroft, S. (1996). ARF and PITP restore GTP S-stimulated protein secretion from cytosol-depleted HL60 cells by promoting PIP2 synthesis. *Curr. Biol.* **6**, 730-738.
Friml, J., Vieten, A., Sauer, M., Weijers, D., Schwarz, H., Hamann, T., Offringa, R. and Jürgens, G. (2003). Efflux-dependent auxin gradients establish the apical-basal axis of Arabidopsis. *Nature* **426**, 147-153.
Hay, J. C. and Martin, T. F. J. (1993). Phosphatidylinositol transfer protein required for ATP-dependent priming of Ca(2+)-activated secretion. *Nature* **366**, 572-575.
Ischebeck, T., Werner, S., Krishnamoorthy, P., Lerche, J., Meijón, M., Stenzel, I., Löfke, C., Wiessner, T., Im, Y. J., Perera, I. Y. et al. (2013). Phosphatidylinositol 4,5-bisphosphate influences PIN polarization by controlling clathrin-mediated membrane trafficking in Arabidopsis. *Plant Cell* **25**, 4894-4911.
Isono, E., Katsiarimpa, A., Müller, I. K., Anzenberger, F., Stierhof, Y.-D., Geldner, N., Chory, J. and Schwechheimer, C. (2010). The deubiquitinating enzyme AMSH3 is required for intracellular trafficking and vacuole biogenesis in Arabidopsis thaliana. *Plant Cell* **22**, 1826-1837.
Jeong, S., Bayer, M. and Lukowitz, W. (2011). Taking the very first steps: From polarity to axial domains in the early Arabidopsis embryo. *J. Exp. Bot.* **62**, 1687-1697.
Kapranov, P., Routt, S. M., Bankaitis, V., De Bruijn, F. J. and Szczyglowski, K. (2001). Nodule-specific regulation of phosphatidylinositol transfer protein expression in Lotus japonicus. *Plant Cell* **13**, 1369-1382.
Karimi, M., Bleys, A., Vanderhaeghen, R. and Hilson, P. (2007). Building blocks for plant gene assembly. *Plant Physiol.* **145**, 1183-1191.
Kearns, M. A., Monks, D. E., Fang, M., Rivas, M. P., Courtney, P. D., Chen, J., Prestwich, G. D., Theibert, A. B., Dewey, R. E. and Bankaitis, V. B. (1998). Novel developmentally regulated phosphoinositide binding proteins from soybean whose expression bypasses the requirement for an essential phosphatidylinositol transfer protein in yeast. *EMBO J.* **17**, 4004-4017.
Kiba, A., Nakano, M., Vincent-Pope, P., Takahashi, H., Sawasaki, T., Endo, Y., Ohnishi, K., Yoshioka, H. and Hikichi, Y. (2012). A novel Sec14 phospholipid transfer protein from Nicotiana benthamiana is up-regulated in response to Ralstonia solanacearum infection, pathogen associated molecular patterns and effector molecules and involved in plant immunity. *J. Plant Physiol.* **169**, 1017-1022.
Kleine-Vehn, J., Dhonukshe, P., Sauer, M., Brewer, P. B., Wiśniewska, J., Paciorek, T., Benková, E. and Friml, J. (2008). ARF GEF-dependent transcytosis and polar delivery of PIN auxin carriers in Arabidopsis. *Curr. Biol.* **18**, 526-531.
Kleine-Vehn, J., Huang, F., Naramoto, S., Zhang, J., Michniewicz, M., Offringa, R. and Friml, J. (2009). PIN auxin efflux carrier polarity is regulated by PINOID kinase-mediated recruitment into GNOM-independent trafficking in Arabidopsis. *Plant Cell* **21**, 3839-3849.
Knox, K., Grierson, C. S. and Leyser, O. (2003). AXR3 and SHY3 interact to regulate root hair development. *Development* **130**, 5769-5777.
Lavy, M. and Estelle, M. (2016). Mechanisms of auxin signaling. *Development* **143**, 3226-3229.
Malamy, J. E. and Benfey, P. N. (1997). Organization and cell differentiation in lateral roots of Arabidopsis thaliana. *Development* **44**, 33-44.
Mei, Y., Jia, W.-J., Chu, Y.-J. and Xue, H.-W. (2012). Arabidopsis phosphatidylinositol monophosphate 5-kinase 2 is involved in root gravitropism through regulation of polar auxin transport by affecting the cycling of PIN proteins. *Cell Res.* **22**, 581-597.
Meijer, H. J. G. and Munnik, T. (2003). Phospholipid-based signaling in plants. *Annu. Rev. Plant Biol.* **54**, 265-306.
Monks, D. E., Aghoram, K., Courtney, P. D., DeWald, D. B. and Dewey, R. E. (2001). Hyperosmotic stress induces the rapid phosphorylation of a soybean phosphatidylinositol transfer protein homolog through activation of the protein kinases SPK1 and SPK2. *Plant Cell* **13**, 1205.
Mousley, C. J., Tyeryar, K. R., Vincent-Pope, P. and Bankaitis, V. A. (2007). The Sec14-superfamily and the regulatory interface between phospholipid metabolism and membrane trafficking. *Biochim. Biophys. Acta* **1771**, 727-736.
Mueller-Roeber, B. and Pical, C. (2002). Inositol phospholipid metabolism in Arabidopsis. Characterized and putative isoforms of inositol phospholipid kinase and phosphoinositide-specific phospholipase C1. *Plant Physiol.* **130**, 22-46.
Nováková, P., Hirsch, S., Feraru, E., Tejos, R., van Wijk, R., Viaene, T., Heilmann, M., Lerche, J., De Rycke, R., Feraru, M. I. et al. (2014). SAC phosphoinositide phosphatases at the tonoplast mediate vacuolar function in Arabidopsis. *Proc. Natl. Acad. Sci. USA* **111**, 2818-2823.
Novick, P. and Schekman, R. (1979). Secretion and cell-surface growth are blocked in a temperature-sensitive mutant of Saccharomyces cerevisiae. *Proc. Natl. Acad. Sci. USA* **76**, 1858-1862.
Novick, P., Field, C. and Schekman, R. (1980). Identification of 23 complementation groups required for post-translational events in the yeast secretory pathway. *Cell* **21**, 205-215.
Novick, P., Ferro, S. and Schekman, R. (1981). Order of events in the yeast secretory pathway. *Cell* **25**, 461-469.
Omelyanchuk, N. A., Kovrizhnykh, V. V., Oshchepkova, E. A., Pasternak, T., Palme, K. and Mironova, V. V. (2016). A detailed expression map of the PIN1 auxin transporter in Arabidopsis thaliana root. *BMC Plant Biol.* **16**, 5.
Ossowski, S., Schwab, R. and Weigel, D. (2008). Gene silencing in plants using artificial microRNAs and other small RNAs. *Plant J.* **53**, 674-690.
Paciorek, T., Zažímalová, E., Ruthardt, N., Petrášek, J., Stierhof, Y.-D., Kleine-Vehn, J., Morris, D. A., Emans, N., Jürgens, G., Geldner, N. et al. (2005). Auxin inhibits endocytosis and promotes its own efflux from cells. *Nature* **435**, 1251-1256.
Peiró, A., Izquierdo-Garcia, A. C., Sanchez-Navarro, J. A., Pallas, V., Mulet, J. M. and Aparicio, F. (2014). Patellins 3 and 6, two members of the Plant Patellin family, interact with the movement protein of Alfalfa mosaic virus and interfere with viral movement. *Mol. Plant Pathol.* **15**, 881-891.
Peterman, T. K., Ohol, Y. M., McReynolds, L. J. and Luna, E. J. (2004). Patellin1, a novel sec14-like protein, localizes to the cell plate and binds phosphoinositides. *Plant Physiol.* **136**, 3080-3094.
Petrášek, J. and Friml, J. (2009). Auxin transport routes in plant development. *Development* **136**, 2675-2688.
Petrášek, J., Mravec, J., Bouchard, R., Blakeslee, J. J., Abas, M., Seifertová, D., Wisniewska, J., Tadele, Z., Kubes, M., Covanová, M. et al. (2006). PIN proteins perform a rate-limiting function in cellular auxin efflux. *Science* **312**, 914-918.
Robert, S., Kleine-Vehn, J., Barbez, E., Sauer, M., Paciorek, T., Baster, P., Vanneste, S., Zhang, J., Simon, S., Čovanová, M. et al. (2010). ABP1 mediates auxin inhibition of clathrin-dependent endocytosis in Arabidopsis. *Cell* **143**, 111-121.
Robert, H. S., Grones, P., Stepanova, A. N., Robles, L. M., Lokerse, A. S., Alonso, J. M., Weijers, D. and Friml, J. (2013). Local auxin sources orient the apical-basal axis in Arabidopsis embryos. *Curr. Biol.* **23**, 2506-2512.
Robert, H. S., Grunewald, W., Sauer, M., Cannoot, B., Soriano, M., Swarup, R., Weijers, D., Bennett, M., Boutilier, K. and Friml, J. (2015). Plant embryogenesis requires AUX/LAX-mediated auxin influx. *Development* 702-711.
Ruiz Rosquete, M., Barbez, E. and Kleine-Vehn, J. (2012). Cellular auxin homeostasis: Gatekeeping is housekeeping. *Mol. Plant* **5**, 772-786.
Ruzicka, K., Simásková, M., Duclercq, J., Petrášek, J., Zazímalová, E., Simon, S., Friml, J., Van Montagu, M. C. E. and Benková, E. (2009). Cytokinin regulates root meristem activity via modulation of the polar auxin transport. *Proc. Natl. Acad. Sci. USA* **106**, 4284-4289.
Sauer, M., Balla, J., Luschnig, C., Wis, J., Reinöhl, V. and Benková, E. (2006). Canalization of auxin flow by Aux/IAA-ARF-dependent feedback regulation of PIN polarity. *Genes Dev.* **20**, 2902-2911.
Sauer, M., Robert, S. and Kleine-Vehn, J. (2013). Auxin: simply complicated. *J. Exp. Bot.* **64**, 2565-2577.
Simon, J.-P., Morimoto, T., Bankaitis, V., Gottlieb, T. A., Ivanov, I. E., Adesnik, M. and Sabatini, D. D. (1998). An essential role for the phosphatidylinositol transfer protein in the scission of coatomer-coated vesicles from the trans-Golgi network. *Proc. Natl. Acad. Sci. USA* **95**, 11181-11186.

Smit, M. E. and Weijers, D. (2015). The role of auxin signaling in early embryo pattern formation. *Curr. Opin. Plant Biol.* **28**, 99-105.

Suzuki, T., Matsushima, C., Nishimura, S., Higashiyama, T., Sasabe, M. and Machida, Y. (2016). Identification of phosphoinositide-binding protein PATELLIN2 as a substrate of Arabidopsis MPK4 MAP kinase during septum formation in cytokinesis. *Plant Cell Physiol.* **57**, 1744-1755.

Tanaka, H., Dhonukshe, P., Brewer, P. B. and Friml, J. (2006). Spatiotemporal asymmetric auxin distribution: a means to coordinate plant development. *Cell. Mol. Life Sci.* **63**, 2738-2754.

Tang, W., Deng, Z., Oses-Prieto, J. A., Suzuki, N., Zhu, S., Zhang, X., Burlingame, A. L. and Wang, Z.-Y. (2008). Proteomics studies of brassinosteroid signal transduction using prefractionation and two-dimensional DIGE. *Mol. Cell. Proteomics* **7**, 728-738.

Tejos, R., Sauer, M., Vanneste, S., Palacios-Gomez, M., Li, H., Heilmann, M., van Wijk, R., Vermeer, J. E. M., Heilmann, I., Munnik, T. et al. (2014). Bipolar plasma membrane distribution of phosphoinositides and their requirement for auxin-mediated cell polarity and patterning in Arabidopsis. *Plant Cell* **26**, 2114-2128.

Ugalde, J.-M., Rodriguez-Furlán, C., De Rycke, R., Norambuena, L., Friml, J., León, G. and Tejos, R. (2016). Phosphatidylinositol 4-phosphate 5-kinases 1 and 2 are involved in the regulation of vacuole morphology during Arabidopsis thaliana pollen development. *Plant Sci.* **250**, 10-19.

van Leeuwen, W., Vermeer, J. E. M., Gadella, T. W. J. and Munnik, T. (2007). Visualization of phosphatidylinositol 4,5-bisphosphate in the plasma membrane of suspension-cultured tobacco BY-2 cells and whole Arabidopsis seedlings. *Plant J.* **52**, 1014-1026.

Vermeer, J. E. M., Van Leeuwen, W., Tobeña-Santamaria, R., Laxalt, A. M., Jones, D. R., Divecha, N., Gadella, T. W. J. and Munnik, T. (2006). Visualization of PtdIns3P dynamics in living plant cells. *Plant J.* **47**, 687-700.

Vincent, P., Chua, M., Nogue, F., Fairbrother, A., Mekeel, H., Xu, Y., Allen, N., Bibikova, T. N., Gilroy, S. and Bankaitis, V. (2005). A Sec14p-nodulin domain phosphatidylinositol transfer protein polarizes membrane growth of Arabidopsis thaliana root hairs. *J. Cell Biol.* **168**, 801-812.

Weijers, D., Schlereth, A., Ehrismann, J. S., Schwank, G., Kientz, M. and Jurgens, G. (2006). Auxin triggers transient local signaling for cell specification in Arabidopsis embryogenesis. *Dev. Cell* **10**, 265-270.

Wiśniewska, J., Xu, J., Seifertová, D., Brewer, P. B., Růžička, K., Blilou, I., Rouquié, D., Benková, E., Scheres, B. and Friml, J. (2006). Polar PIN localization directs auxin flow in plants. *Science* **312**, 883.

Xue, H., Chen, X. and Li, G. (2007). Involvement of phospholipid signaling in plant growth and hormone effects. *Curr. Opin. Plant Biol.* **10**, 483-489.

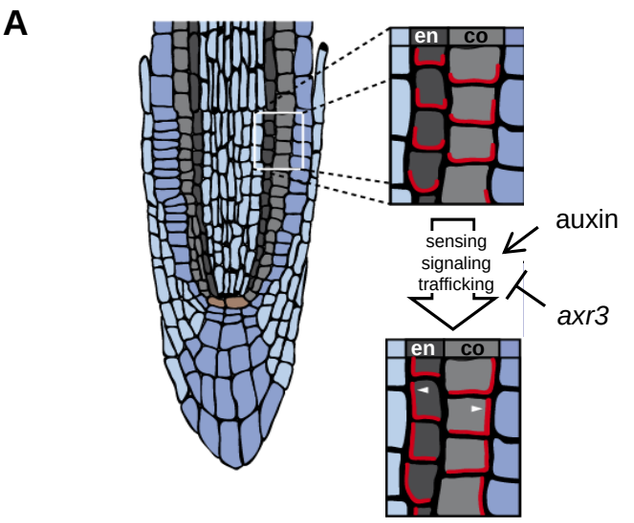

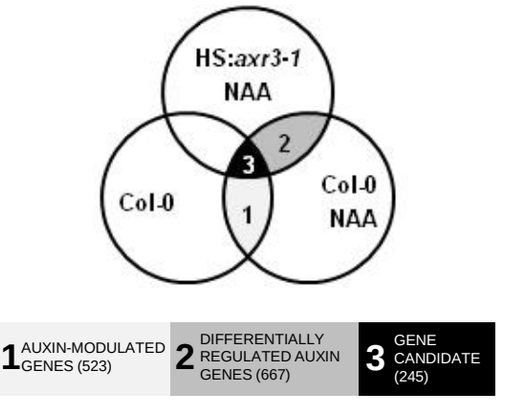

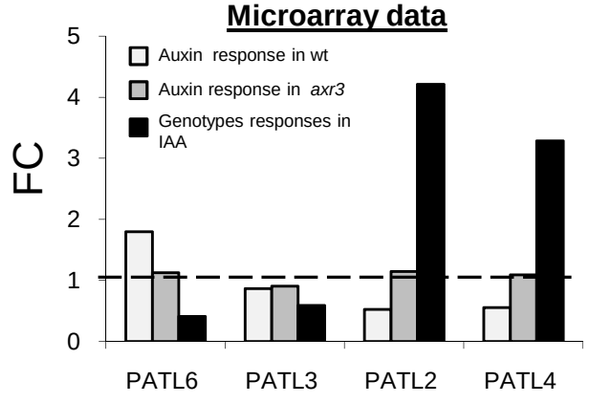

D

		Auxin response in wt		Auxin response in *axr3*		Genotypes response in IAA	
Gene	ATI code	FC	*P value*	FC	*P value*	FC	*P value*
PATL2	AT1G22530	**0.547**	**0.003**	1.121	0.468	**3.701**	**0.000**
PATL3	AT1G72160	0.868	0.291	0.881	0.341	**0.594**	**0.003**
PATL4	AT1G30690	**0.623**	**0.003**	1.123	0.353	**2.952**	**0.000**
PATL6	AT3G51670	**1.753**	**0.006**	1.075	0.653	**0.422**	**0.000**

Figure S1. Microarray for auxin effect on PIN lateralization identifies PATELLINS as candidate genes.
A. PIN1 and PIN2 are basally localized in endodermis and young cortex cells, respectively, pumping auxin in the direction of the root tip. Auxin is able to modify PIN1 and PIN2 localization to baso-lateral. This effect is dependent on the AXR3-mediated transcription of so far unknown components.
B. Microarray results. Among the auxin-regulated genes in wild type, we selected 245 gene candidates as being auxin inducible but differentially expressed in the dominant negative version of AXR3 (HS:*axr3-1*).
C, D. PATELLINs are auxin-regulated genes in an AXR3-dependent fashion. PATL6 is auxin inducible depending on AXR3. On the other hand, PATL2 and PATL4 are negatively regulated by auxin and in the HS:*axr3-1* mutant background these effects were lost. In D, the Fold Change (FC) and the *P* values for the *PATL* genes obtained in the microarray data.

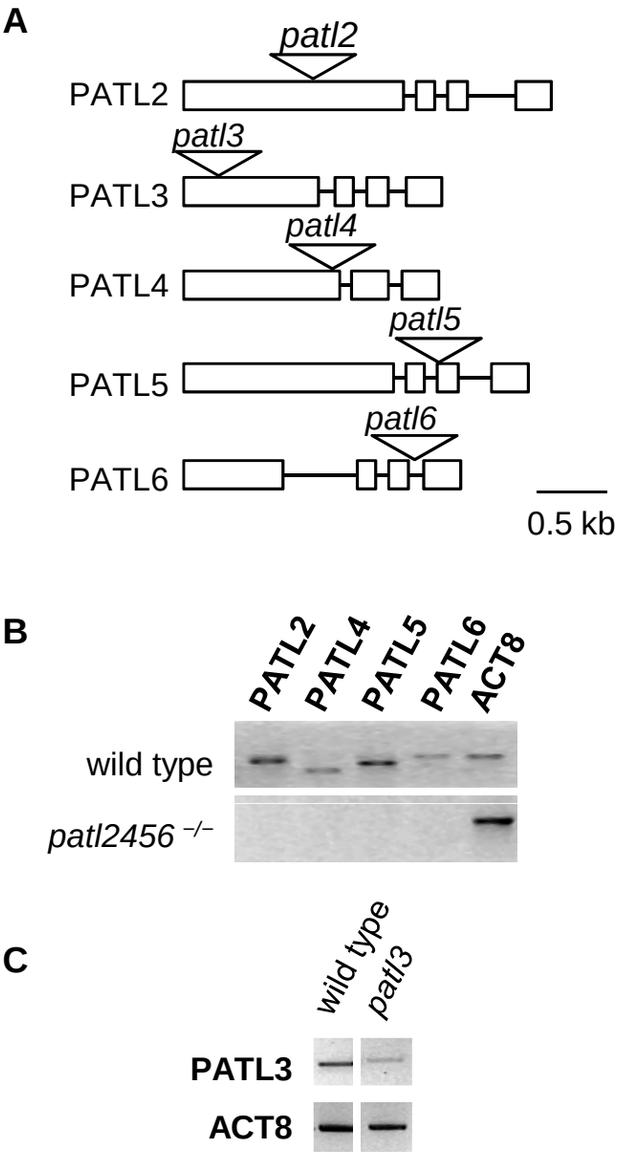

Figure S2. PATELLIN quadruple mutant *patl2456*$^{-/-}$

A-C. Scheme of *PATL* genes representing exons (boxes) and introns (lines) and the insertion sites of the T-DNA insertions in the *patl* mutants (A). RT-PCR analysis for *PATL* gene expression in wild type and *patl2456*$^{-/-}$ quadruple knockout mutants (B) and *patl3* knockdown mutant (C).

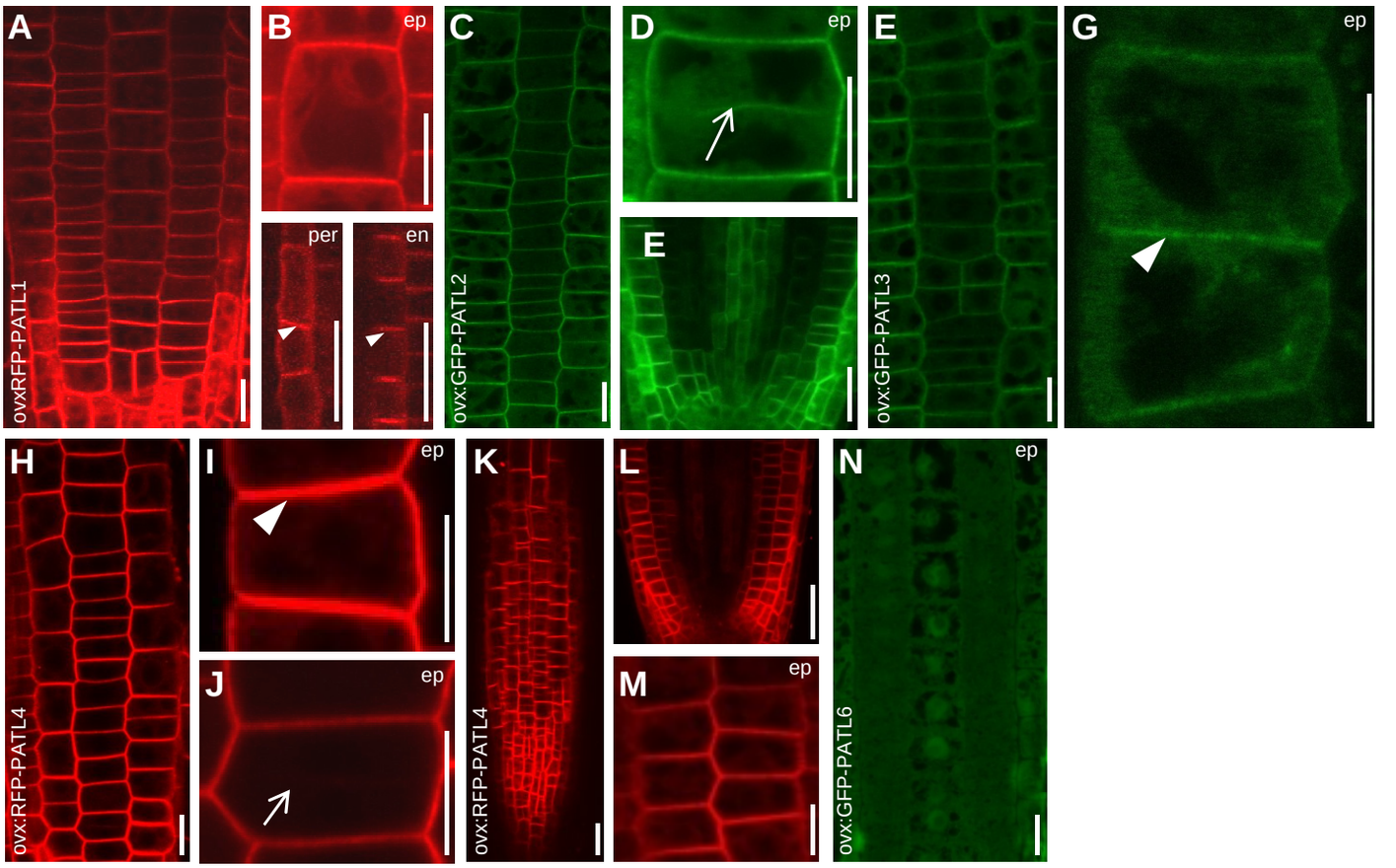

Figure S3. PATELLIN localization in FP-PATL overexpressors lines.
FP-PATL1-5 are localized at the PM or cell plates, and GFP-PATL6 is accumulated at PATL localization was observed in primary roots in GFP-PATL (C to G, N) or RFP-PATL (A, B, H to L) reporter lines expressed in wild type plants using the Cauliflower mosaic virus 35S promoter. Arrowheads are used to highlight asymetric localization at plasma membranes (B, G), arrowheads depict asymmetric PATL localization at the plasma membrane (C, I, J, O) and arrows indicate cell plate localized PATLs (D, H). . All images are representative of at least 20 different individuals. Bar size= 20 µm.

Table S1. Candidates genes differentially regulated in *HS::axr3-2* compared to auxin-regulated genes in wild type. The gene model description is depicted as it appears in TAIR database. In bold are indicated the candidates that were tested for defects on PIN polarity.

Click here to Download Table S1

Table S2. Sec14-like proteins in *Arabidopsis*.

		Sec14p homology			
Gene model	**ATI code**	**Identities**	**+**	**E value**	**Other protein domains**
AtSFH1/COW1	AT4G34580	102/242	152/242	1e-53	Nodullin[a]
AtSFH2	AT4G39180	102/236	146/236	2e-53	Nodullin[a]
AtSFH3	AT2G21540	104/250	150/250	1e-52	Nodullin[a]
AtSFH4	AT1G19650	103/241	150/241	1e-51	Nodullin[a]
AtSFH5	AT1G75370	101/241	147/241	3e-48	Nodullin[a]
AtSFH6	AT4G39170	97/239	149/239	1e-50	Nodullin[a]
AtSFH7	AT2G16380	102/248	149/248	1e-49	Nodullin[a]
AtSFH8	AT2G21520	97/243	150/243	7e-49	Nodullin[a]
AtSFH9	AT3G24840	100/242	141/242	2e-47	Nodullin[a]
AtSFH10	AT2G18180	89/232	140/232	1e-47	Nodullin[a]
AtSFH11	AT5G47510	95/236	133/236	2e-46	ND
AtSFH12	AT4G36490	91/243	146/243	4e-47	Nodullin[a]
AtSFH13	AT1G55690	90/237	141/237	5e-40	Nodullin[a]
AtSFH14	AT5G56160	90/236	142/236	4e-43	ND
PATL1	AT1G72150	58/221	100/221	2e-11	GOLD; CRAL/Trio
PATL2	AT1G22530	69/221	103/221	3e-11	GOLD; CRAL/Trio
PATL3	AT1G72160	62/216	106/216	4e-17	GOLD; CRAL/Trio
PATL4	AT1G30690	68/224	106/224	2e-16	GOLD; CRAL/Trio
PATL5	AT4G09160	62/217	101/217	2e-15	GOLD; CRAL/Trio
PATL6	AT3G51670	68/232	102/232	1e-14	GOLD; CRAL/Trio
AtPITPs	AT4G36640	75/254	116/254	9e-18	-
	AT5G47730	60/209	99/209	2e-16	-
	AT1G55840	62/209	98/209	4e-16	-
	AT1G01630	66/218	98/218	1e-15	-
	AT1G75170	67/217	102/217	4e-15	-
	AT1G22180	31/96	56/96	7e-08	-
	AT4G08690	56218	97/218	2e-10	-
	AT1G14820	54/222	96/222	2e-08	-
	AT3G46450	54/213	86/213	2e-06	-
	AT1G05370	41/182	79/182	5e-05	-
	AT5G63060	52/214	88/214	2e-03	-
	AT3G22410	39/183	85/183	5e-04	-

Table S3. Segregation of *patl2* mutant allele in *the progeny of a single patl2* $^{+/-}$ *3456* $^{-/-}$ mutant plant.

patl2	n_O	f_O	n_E	f_E	
+ / +	14	0.1944	18	0.25	$\chi^2 = 13.861$
+ / −	51	0.7083	36	0.5	$p = 0.001$
− / −	7	0.0972	18	0.25	
TOTAL	**72**	**1**	**72**	**1**	

$n_O$observed amount; f_O observed frequency; $n_E$expected amount; f_E expected frequency. Expected values under the assumption of Mendelian traits and no linkage among the different alleles.

Table S4. List of primers used for cloning procedures, patl mutant genotyping, amiRNA construct and transcripts level analysis.

Gene	Sequence	Orientation	Application
PATL1	ATGGCTCAAGAGGAAGTAC	Fw	Cloning coding sequence, RT-PCR
PATL1	AGTTTTGAACCTGTAGTAG	Rv	Cloning coding sequence, RT-PCR
PATL2	ATGGCTCAAGAAGAGATAC	Fw	Cloning coding sequence, RT-PCR
PATL2	TGCTTGGGTTTTGGACCTG	Rv	Cloning coding sequence, RT-PCR
PATL3	ATGGCTGAAGAACCTACTAC	Fw	Cloning coding sequence, RT-PCR
PATL3	GAGAGGTTTGACATTGAAC	Rv	Cloning coding sequence, RT-PCR
PATL4	ATGACTGCTGAAGTTAAGG	Fw	Cloning coding sequence, RT-PCR
PATL4	GGAAGAGGATTCAGTCTTG	Rv	Cloning coding sequence, RT-PCR
PATL5	ATGTCTCAAGATTCTGCAAC	Fw	Cloning coding sequence, RT-PCR
PATL5	CTCACAAGCTAAAGGCTTA	Rv	Cloning coding sequence, RT-PCR
PATL6	ATGGATGCTTCATTGTCTCC	Fw	Cloning coding sequence, RT-PCR
PATL6	GACGGTTGTAGTAGATTTCCGG	Rv	Cloning coding sequence, RT-PCR
ACTIN8	ACCTTGCTGGTCGTGACCTTACTG	Fw	RT-PCR
ACTIN8	GATCCCGTCATGGAAACGATGTCTC	Rv	RT-PCR
PATL1	GGATTTTTAACGGATCACTC	Fw	Promoter sequence cloning
PATL1	CTTTCTTGTCTGATTTTAGA	Rv	Promoter sequence cloning
PATL2	TCCGGTTTGACTGGATTTTT	Fw	Promoter sequence cloning
PATL2	GATCACTTGATTCGAAAGGG	Rv	Promoter sequence cloning
PATL3	TTTTTACTTGTGCCGTCTTG	Fw	Promoter sequence cloning
PATL3	GCAGGTTTAGGAAACAATTC	Rv	Promoter sequence cloning
PATL4	ATAACTGTTGACTTCAACTA	Fw	Promoter sequence cloning
PATL4	CTTAAAGCCTGTCATTCAGA	Rv	Promoter sequence cloning
PATL5	CCCTAATTCACATTGGTC	Fw	Promoter sequence cloning
PATL5	TTTTTTATTGTTCTTGAA	Rv	Promoter sequence cloning
PATL6	TATTTAGCCATAGTGGAAAG	Fw	Promoter sequence cloning
PATL6	TGTTTCTTGAGAGTTTTTC	Rv	Promoter sequence cloning
PATL2	GGAAAAATCTCTTGAGGCTGAA	Right	Genotyping *patl* mutants
PATL2	CTTGTTTGTCGACACCGTGAG	Left	Genotyping *patl* mutants
PATL3	GTCATTGGATCCAATTTCACG	Right	Genotyping *patl* mutants
PATL3	AACCTTCTCAAGATCATCCAC	Left	Genotyping *patl* mutants
PATL4	TCTACTGTTTTGAACCCACCG	Right	Genotyping *patl* mutants
PATL4	CTGAGGCTGTTGTTACCGAAG	Left	Genotyping *patl* mutants
PATL5	TTTGTAGCTGGTGGTGTTTCC	Right	Genotyping *patl* mutants
PATL5	GGCTTTTGTTACTCACAAGC	Left	Genotyping *patl* mutants
PATL6	CAAACCCAAGAAAGAAAACCC	Right	Genotyping *patl* mutants
PATL6	ATTTGTGCGGTTTCTTGAG	Left	Genotyping *patl* mutants
LBb1+	ATTTTGCCGATTTCGGAAC		Genotyping *patl* mutants
LBa1	TGGTTCACGTAGTGGGCCATCG		Genotyping *patl* mutants
PATL1	gaTATAGTGTAGTTTGCTGGCGGtctctcttttgtattcc	miR-s	amiRNAa
PATL1	gaCCGCCAGCAAACTACACTATAtcaaagagaatcaatga	miR-a	amiRNAa
PATL1	gaCCACCAGCAAACTTCACTATTtcacaggtcgtgatatg	miR*s	amiRNAa
PATL1	gaAATAGTGAAGTTTGCTGGTGGtctacatatatattcct	miR*a	amiRNAa
PATL1	gaTCGAATTGTTTAACAGCCCGTtctctcttttgtattcc	miR-s	amiRNAb
PATL1	gaACGGGCTGTTAAACAATTCGAtcaaagagaatcaatga	miR-a	amiRNAb
PATL1	gaACAGGCTGTTAAAGAATTCGTtcacaggtcgtgatatg	miR*s	amiRNAb
PATL1	gaACGAATTCTTTAACAGCCTGTtctacatatatattcct	miR*a	amiRNAb
PATL3	gaTGTCTTATTATAAAGCTCCGTtctctcttttgtattcc	miR-s	amiRNAa
PATL3	gaACGGAGCTTTATAATAAGACAtcaaagagaatcaatga	miR-a	amiRNAa
PATL3	gaACAGAGCTTTATATTAAGACTtcacaggtcgtgatatg	miR*s	amiRNAa
PATL3	gaAGTCTTAATATAAAGCTCTGTtctacatatatattcct	miR*a	amiRNAa
PATL3	gaTACACATAAGATATCTCGCTTtctctcttttgtattcc	miR-s	amiRNAb
PATL3	gaAAGCGAGATATCTTATGTGTAtcaaagagaatcaatga	miR-a	amiRNAb
PATL3	gaAAACGAGATATCTAATGTGTTtcacaggtcgtgatatg	miR*s	amiRNAb
PATL3	gaAACACATTAGATATCTCGTTTtctacatatatattcct	miR*a	amiRNAb